Molecular Biology of the Cell
Vol. 12, 4054–4065, December 2001

Microtubule Flux Mediates Poleward Motion of Acentric Chromosome Fragments during Meiosis in Insect Spermatocytes[V]

James R. LaFountain, Jr.,*† Rudolf Oldenbourg,‡ Richard W. Cole,§ and Conly L. Rieder§‖

*Department of Biological Sciences, University at Buffalo, Buffalo, New York 14260; ‡Marine Biological Laboratory, Woods Hole, Massachusetts 02543; §Laboratory of Cell Regulation, Division of Molecular Medicine, Wadsworth Center, New York State Department of Health, Albany, New York 12201-0509; and ‖Department of Biomedical Sciences, State University of New York, Albany, New York 12222

Submitted May 15, 2001; Revised July 27, 2001; Accepted September 10, 2001
Monitoring Editor: Ted Salmon

We applied a combination of laser microsurgery and quantitative polarization microscopy to study kinetochore-independent forces that act on chromosome arms during meiosis in crane fly spermatocytes. When chromosome arms located within one of the half-spindles during prometa- or metaphase were cut with the laser, the acentric fragments (lacking kinetochores) that were generated moved poleward with velocities similar to those of anaphase chromosomes (~0.5 μm/min). To determine the mechanism underlying this poleward motion of detached arms, we treated spermatocytes with the microtubule-stabilizing drug taxol. Spindles in taxol-treated cells were noticeably short, yet with polarized light, the distribution and densities of microtubules in domains where fragment movement occurred were not different from those in control cells. When acentric fragments were generated in taxol-treated spermatocytes, 22 of 24 fragments failed to exhibit poleward motion, and the two that did move had velocities attenuated by 80% (to ~0.1 μm/min). In these cells, taxol did not inhibit the disjunction of chromosomes nor prevent their poleward segregation during anaphase, but the velocity of anaphase was also decreased 80% (~0.1 μm/min) relative to untreated controls. Together, these data reveal that microtubule flux exerts pole-directed forces on chromosome arms during meiosis in crane fly spermatocytes and strongly suggest that the mechanism underlying microtubule flux also is used in the anaphase motion of kinetochores in these cells.

INTRODUCTION

The poleward motion of a chromosome during mitosis or meiosis coincides with the shortening of its associated kinetochore fiber microtubules. Recent investigations on this motion have focused on determining the site(s) where kinetochore microtubule disassembly occurs, as well as on how the force for motion is generated. Two general models have arisen from these studies. In the "Pac-man" model, the kinetochore powers chromosome poleward motion, which occurs along kinetochore microtubules that shorten by subunit removal at the kinetochore (reviewed in Rieder and Salmon, 1994). In this model kinetochore-associated minus end-directed motors, such as cytoplasmic dynein, are envisioned to provide the force for chromosome movement, although it could also be generated by the disassembly of kinetochore microtubule plus ends within the kinetochore (Inoue and Salmon, 1995). Such a model is supported by the facts that dynein is present at kinetochores (Pfarr *et al.*, 1990; Steurer *et al.*, 1990; reviewed in Hoffman *et al.*, 2001) and that its depletion attenuates the rate of poleward chromosome motion (Savoian *et al.*, 2000; Sharp *et al.*, 2000).

Alternatively, in the "traction fiber" model, the chromosome is dragged poleward by the poleward motion of its associated kinetochore microtubules that shorten by subunit removal at the pole (reviewed in Pickett-Heaps *et al.*, 1996). In this model, force production is envisioned to occur, for example, as plus end-directed motors anchored within the spindle matrix interact with and push all spindle microtubules poleward (Mitchison and Sawin, 1990; Sawin and Mitchison, 1991). This model is supported by microinjection (Mitchison *et al.*, 1986) and photoactivation studies (Mitchison, 1989), which reveal a "flux" of tubulin subunits that are constantly incorporated before anaphase into the plus ends

[V] Online version of this article contains video material for certain figures. Online version available at www.molbiolcell.org.

† Corresponding author: E-mail address: jrl@acsu.buffalo.edu.

of microtubules while being removed from their minus ends within the pole. The flux mechanism exerts a poleward force on the chromosome when subunit incorporation at the kinetochore ceases, as occurs at anaphase onset (Waters *et al.*, 1998).

The relative contribution that each of these mechanisms makes to the poleward motion of a chromosome appears to depend on the system. The rate that kinetochore microtubules move poleward in spindles formed in *Xenopus* oocyte extracts is the same as the rate exhibited by the chromosomes at anaphase (Desai *et al.*, 1998). This suggests that poleward motion in this in vitro system is powered entirely by flux. In contrast, in vertebrate somatic cells (Mitchison and Salmon, 1992; Zhai *et al.*, 1995), both mechanisms appear to operate simultaneously, but the contribution made by flux is much less (~15–35%) than that made by the poleward movement of kinetochores.

In addition to those forces that act on kinetochores, the chromosome arms are also subjected to spindle-mediated forces throughout the division process. In vertebrate somatic cells, when the arm of a prometaphase chromosome positioned near a pole is severed from the kinetochore, it is ejected away from the pole (reviewed in Rieder and Salmon, 1994). The "polar wind" propelling that motion appears to be mediated by plus end-directed motors associated with the chromosome arms (i.e., chromokinesin; Antonio *et al.*, 2000; Funabiki and Murray, 2000). In contrast, when a pole-directed arm of a metaphase chromosome during plant (*Hemanthus*) mitosis is similarly severed from its kinetochore, it is transported poleward at the same velocity exhibited by chromosomes during anaphase (Khodjakov *et al.*, 1996). The force-producing mechanism behind this motion remains to be determined, but candidates include microtubule flux or chromosome-associated minus end-directed motors.

Insect spermatocytes have long been a popular system for studying the forces that move and position chromosomes. In crane fly spermatocytes, chromosome arms sometimes become aligned parallel to the spindle long axis during spindle formation, and maintain this alignment throughout anaphase (Adames and Forer, 1996). This suggests that in insect spermatocytes, as in plant mitosis, poleward forces act along the length of the chromosome independent of those acting on the kinetochore. To directly test this hypothesis we used laser microsurgery to sever chromosome fragments lacking kinetochores (i.e., acentric fragments) from pole-directed arms. As predicted, these fragments were invariably transported poleward at a velocity (~0.5 μm/min) similar to that exhibited by the kinetochore regions on anaphase chromosomes. We then investigated the mechanism responsible for this motion by repeating our experiments on cells treated with paclitaxel (taxol), a drug that inhibits microtubule flux (Derry *et al.*, 1995; Waters *et al.*, 1996) but not microtubule-dependent motor activity (Vale *et al.*, 1985). In taxol, the poleward movement of acentric fragments was dramatically inhibited: <10% of the fragments generated during metaphase exhibited motion, and in those that did, velocity was greatly attenuated. From these findings we conclude that the poleward force that acts on the chromosome arms in these spermatocytes is generated by microtubule flux and not by molecular motors associated with the chromosome. Furthermore, because taxol treatment similarly attenuated the velocity of poleward chromosome motion during anaphase, it also is mediated largely by flux, as originally suggested by Wilson *et al.* (1994).

MATERIALS AND METHODS

Spermatocyte Culture and Drug Treatment

Spermatocytes were obtained from fourth instars of the crane fly, *Nephrotoma suturalis*, and were prepared for microscopy by rupturing the contents of testes, isolated in tricine insect (TI) buffer (Begg and Ellis, 1979), under oil on the surface of a coverslip attached to a well slide (Janicke and LaFountain, 1986).

Taxol (Sigma, St. Louis, MO) was dissolved in dimethyl sulfoxide (DMSO) at a concentration of 10 mM and stored at −20°C. For treatment of spermatocytes, the above-mentioned stock solution was diluted in TI buffer to obtain the desired concentration (100 nM-50 μM), and isolated testes were incubated in the various dilutions for 15 min to 1 h. During that incubation, taxol was taken up into the testicular fluid surrounding spermatocytes, as well as by spermatocytes that were suspended in that fluid. The concentration of taxol in the testicular fluid was not known; however, the effect of taxol on spermatocytes was evident in the taxol phenotype (see RESULTS) that was achieved. After incubation in taxol-TI buffer, testes were then ruptured under oil for microscopy. Under oil, spermatocytes remained suspended in testicular fluid that contained taxol. Typically, it took 0.5–2 h after cells were prepared for microscopy to find a cell suitable for either microsurgery or analysis of anaphase velocities. Thus, in some cases, results were obtained from cells that had spindles before taxol exposure, and they shortened during exposure. In other cells, nuclear envelope breakdown occurred during exposure to taxol and thus, short spindles were assembled in the presence of taxol. Microsurgical operations were performed on both types, and similar results were obtained

Fluorescence and Phase Contrast Microscopy

For analyzing the position of chromosome arms, testes were fixed with 3% paraformaldehyde, stained with Hoechst 33342 (Sigma) according to methods described previously (LaFountain *et al.*, 1999), and then viewed with a Nikon Optiphot equipped with quad fluor optics and a SPOT 1 digital camera (Diagnostic Instruments, Sterling Heights, MI). For analysis of the progression of cells through the first meiotic division after taxol treatment, living spermatocyte cultures were prepared as described above and monitored with a Zeiss IM35 inverted microscope equipped with phase contrast optics (40×/0.65 numerical aperture objective).

Polarization Microscopy

Images of spindle birefringence were obtained with a polarization microscope, equipped with a universal compensator (CRI, Woburn, MA) that was constructed and operated as described by Oldenbourg and Mei (1995) and then stored as TIFF files that were imported into Image J for analysis (Image J is public-domain software for image analysis available online from NIH Image http://rsb.info.nih.gov/ij/). For quantitative analysis of the birefringence of spindle microtubules, the magnitude of retardance was determined either 1) within selected areas of images of half-spindles, nearby chromosome arms; or 2) from line scans that were made on images either parallel or perpendicular to the spindle axis, again within half-spindles in the vicinities of chromosome arms. With our system, retardance magnitude is proportional to the gray scale (brightness) level within the area of interest of a captured image. To quantify retardance, we simply multiplied the retardance maximum times the fraction of that maximum represented in the area of interest. For example, the line scan in Figure 4G passes through three kinetochore bundles, the brightest of which (left-most in the figure) had a brightness level of 201. That brightness corresponds to a retardance of 2.36 nm (201/255 × 3 nm), because maximal retar-

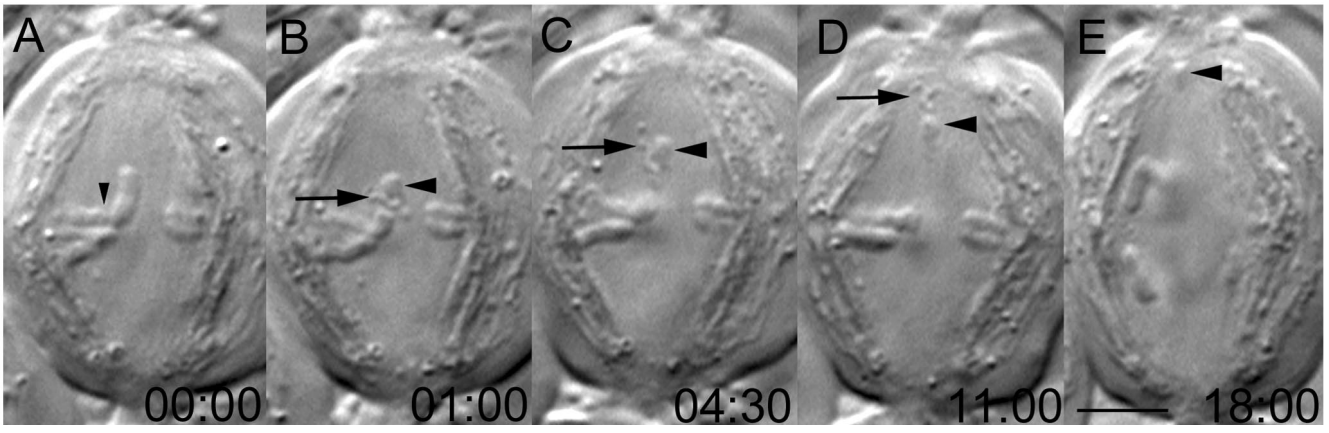

Figure 1. Chromosome fragments lacking kinetochores are transported poleward. Selected frames from a time-lapse recording of a secondary (meiosis II) spermatocyte in which one of the noncoherent pole-directed arms of a dyad (B, large arrowhead) was severed (B) from the kinetochore region (A, small arrowhead). This operation created a sniglet of denatured material (B–D, large arrow) and an acentric chromosome fragment (B–E, large arrowhead). Note that both the sniglet and the acentric fragment moved poleward, and their velocities were similar to those of the kinetochores during anaphase. Time in minutes:seconds. Bar (in E), 5 μm.

dance in this image was 3 nm with a maximum brightness value of 255. Student's *t* test (Microsoft Excel) was used to compare retardance data obtained from taxol-treated and control cells.

Laser Microsurgery and Video Light Microscopy

All operations were conducted on a custom designed video-LM/laser microsurgery workstation described in detail elsewhere (Cole *et al.*, 1995; Khodjakov *et al.*, 1996). In brief, the 1064-nm output of a Q-switched, pulsed (5–7 ns at 10 Hz) Nd:YAG laser (Continuum, Santa Clara, CA) was frequency doubled to 532 nm, filtered, attenuated, and then steered into the epi-port of a Nikon Diaphot 200 de Senarmont compensation Nomarski DIC LM. Each pulse contained ~3 μJ of power at the entry port of the microscope. Chromosome arms required 2–3 s (20–30 laser pulses) to cut and there was no detectable adverse effect of the laser operation on cell viability. In fact, of the 13 spermatocytes monitored after surgery during metaphase or anaphase of meiosis I, all progressed through interkinesis and completed meiosis II ~3 h after irradiation.

Digital images were captured on the laser LM workstation with the use of a Micromax charge-coupled device camera (RSP Princeton Instruments, Trenton, NJ), at 2 frames/min, and the illumination was shuttered between framing intervals. Time-lapse sequences were processed and stored as TIFF files on the hard drive with the use of ImagePro software (Media Cybernetics, Silver Springs, MD) running on a PC. They were then imported into Image J for movie making and further analyses.

Velocity Measurements

To determine the velocities of chromosomes and acentric fragments, Image J software was used to measure the distance from either the center of chromosome fragment or the leading kinetochore of a segregating chromosome to a reference point at either the spindle pole or the spindle equator. These distances, obtained from sequential images, were then plotted as a function of time with the use of Microsoft Excel. Student's *t* test (Microsoft Excel) was used to compare velocities between control and taxol-treated cells. The basal bodies of the polar flagella provided a well-defined reference at the spindle pole; when the plane of the spindle equator was used as the reference, the positions of chromosomes on the metaphase plate and the shape of the mitochondrial sheath outlining the spindle provided the basis for defining that plane.

RESULTS

Among males of *N. suturalis*, the karyotype includes three pairs of metacentric autosomes and two small telocentric sex chromosomes (X and Y). The autosomes pair into three bivalents for meiosis; sex chromosome behavior during meiosis is complicated. X and Y initially pair but then precociously separate into univalents for meiosis I; sex chromosomes behave normally as dyads during meiosis II. The spindle in spermatocytes is well defined, outlined by a sheath, or mantle, of aligned mitochondria (LaFountain, 1972).

Chromosome Arms in Crane Fly Spermatocytes Frequently Become Aligned Parallel to Spindle Long Axis

During spindle formation in both primary and secondary spermatocytes, one of the arms of a chromosome sometimes appears to extend along the spindle toward a pole. This is a particularly prevalent feature of meiosis II, when the arms of the two chromatids comprising a dyad are no longer coherent (Figure 1A). In a survey of fixed spermatocytes from eight testes one-third (78/222) of the metaphase II cells had one or more pole-directed arms. Although considerably less common, pole-directed arms are also found among the nonchiasmic arms of monochiasmic metaphase I bivalents (Figure 2A): of the 277 monochiasmic bivalents in the 247 metaphase I spermatocytes identified in the above-mentioned survey, 11 (4%) had a pole-directed arm (like that depicted in Figure 2A). As previously noted by others (Adames and Forer, 1996), pole-directed arms seen during metaphase often remain pole-directed during anaphase.

Acentric Chromosome Fragments Generated Near the Spindle Equator during Metaphase and Anaphase Are Transported Poleward

To test the hypothesis that the extension of a chromosome arm along the interpolar spindle axis in crane fly spermato-

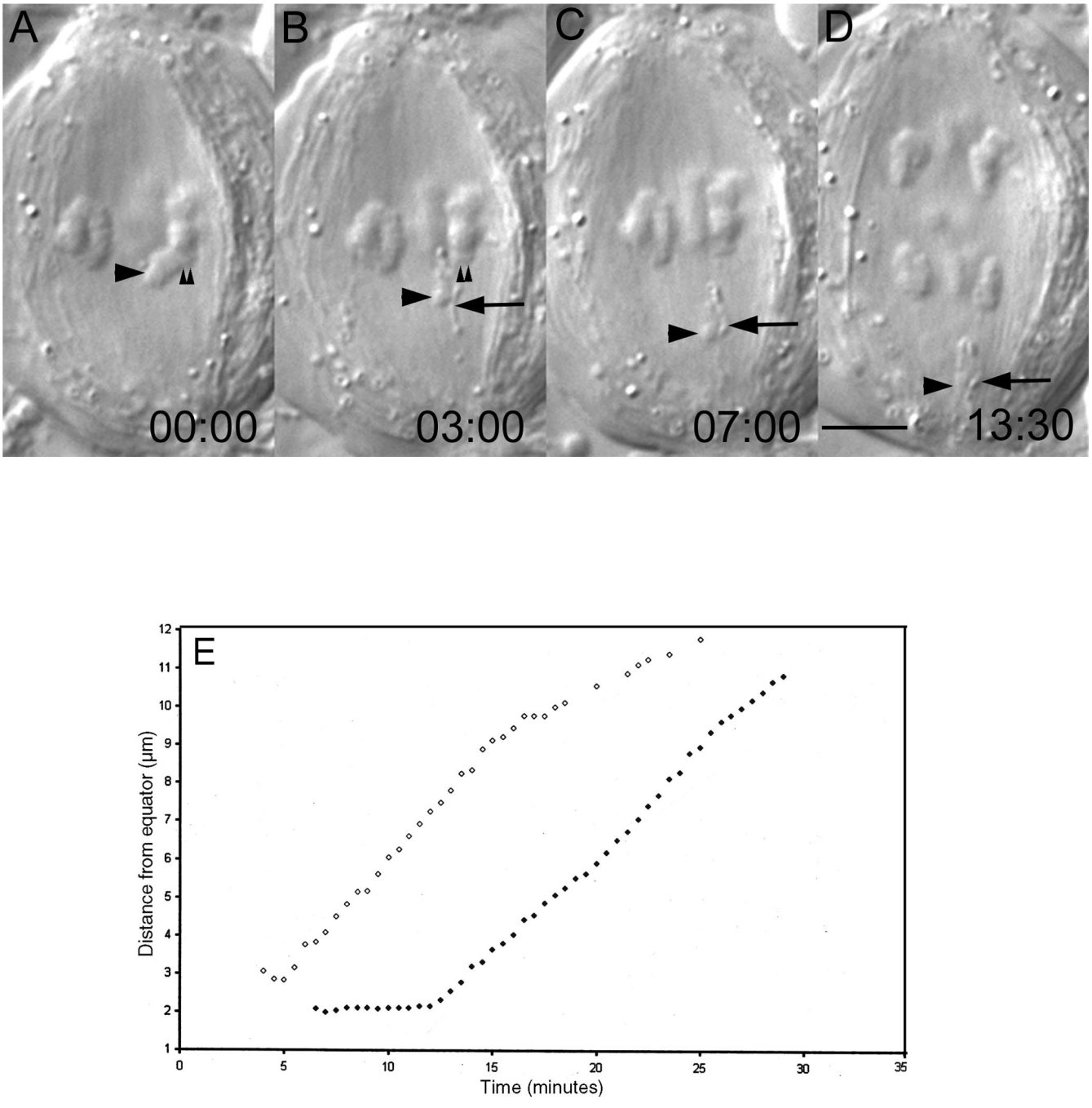

Figure 2. Chromosome fragments lacking kinetochores are transported poleward. (A–D) Selected frames from a time-lapse recording of a primary (meiosis I) spermatocyte in which a pole-directed arm (A, large arrowhead) was severed (B) from the kinetochore region (A and B, small arrowheads) of a monochiasmic bivalent. This operation created a sniglet (B–D, large arrow) and an acentric chromosome fragment (B–D, large arrowhead). As in metaphase II (Figure 1), both the sniglet and acentric fragment moved poleward (D). Time in minutes:seconds. Bar (in D), 5 μm. (E) Distance from the equator versus time for the acentric fragment (○) depicted by the arrowhead in B–D, and also for the lower left half-bivalent (●) in D as it moved poleward during anaphase. Note that each moved with a similar kinetic profile.

cytes is due to a poleward force acting along the arms, we severed the arms from metaphase I and II chromosomes between their kinetochore and telomere regions (Figures 1B and 2B, large arrowheads). In all cases, the resultant acentric fragment was transported poleward with a relatively constant and uniform velocity (Figure 2E), averaging ~0.5 μm/

Table 1. Comparison of spindle organization, transport velocities, and the duration of meiosis 1 in control and taxol-treated spermatocytes

	Untreated	DMSO controls[a]	Taxol-treated[b]
Average interpolar distance at metaphase I	26 ± 0.4 μm (n = 18)	26.6 ± 0.3 μm (n = 7)	15.5 ± 0.3 μm (n = 10)
Average kinetochore-to-pole distance at metaphase I	10.6 ± 0.1 μm (n = 18)	11.4 ± 0.2 μm (n = 10)	6.6 ± 0.2 μm (n = 20)
Average chromosome velocity during anaphase I	~0.5 μm/min (n = 14) (range: 0.3–0.7 μm/min)	~0.5 μm/min (n = 4) (range: 0.5–0.6 μm/min)	~0.1 μm/min (n = 20) (range: 0.1–0.3 μm/min)
Average poleward velocity of acentric fragments generated at metaphase I	~0.5 μm/min (n = 23) (range: 0.3–0.7 μm/min)	~0.5 μm/min (n = 3) (range: 0.4–0.8 μm/min)	no motion (n = 24) ~0.1 μm/min (n = 2)
Average poleward velocity of sniglets generated at metaphase I	~0.5 μm/min (n = 11) (range: 0.3–0.7 μm/min)	~0.5 μm/min (n = 3) (range: 0.4–0.6 μm/min)	no motion (n = 23) ~0.2 μm/min (n = 1)
Average duration between NEB and anaphase I onset	83 min (n = 83) (range: 59–129 min)	72 min (n = 64) (range: 45–92 min)	112 min (n = 167) (range: 78–166 min)

[a] Spermatocytes from testes incubated for 15 min in buffered saline containing 0.05–0.1% DMSO.

[b] Spermatocytes from testes incubated for 15 min in buffered saline containing 5–10 μM taxol and 0.05–0.1% DMSO.

min (range 0.3–0.7 μm/min; n = 23; Table 1). It should be noted here that the kinetochore regions also moved poleward at a similar constant velocity averaging ~0.5 μm/min during anaphase I and II (Figure 2E and Table 1).

A thin linear ribbon of highly refractive material is generated in the cutting plane as the specimen is translated slowly through the focused laser beam (Figure 1B and 2B). These "sniglets" (Cole *et al.*, 1995) can be formed at will, anywhere within the spindle or cell, and presumably consist of material denatured by the laser pulses. As chromosome arms were severed, conspicuous sniglets were formed, and these were also always transported poleward with a velocity similar to that exhibited by the adjacent acentric fragment (Figures 1, C–E, and 2, C and D, arrows; Table 1). When sniglets were formed by irradiating a region of the half-spindle that lacked chromosomes, they were also transported poleward with a velocity similar to that exhibited by acentric fragments and anaphase chromosomes (our unpublished data).

When acentric chromosome fragments were generated at metaphase in a fully formed spindle, they moved in a linear manner into the proximal pole (Figures 1, B–E, and 2, C and D). When generated in early- to mid-prometaphase cells, fragments frequently exhibited a gradual lateral displacement toward the sheath of mitochondria surrounding the spindle as they moved poleward (Figure 3). Thus, in addition to experiencing pole-directed forces, during spindle formation the chromosomes are also subjected to forces directed perpendicular to the spindle long axis that tend to eliminate them laterally from the central domain of the spindle. These so-called "transverse equilibrium forces" were originally described by Östergren (1945), and likely represent the tendency of highly ordered dynamic microtubule arrays to sterically eliminate larger inclusions as they form (see examples in Tucker, 1977).

Taxol Treatment Induces Spindle Shortening, but Does not Prevent Either Anaphase Onset or Poleward Chromosome Motion in Crane Fly Spermatocytes

To investigate the possible contribution made by microtubule flux to the poleward motion of acentric fragments, we treated testes with various concentrations of taxol before making spermatocyte preparations (see MATERIALS AND METHODS). Incubating testes in 5 or 10 μM taxol for 15 min before making cell preparations produced spermatocytes containing spindles that were ~40% shorter than normal (Figure 4C and Table 2), and their spindle poles were broader than normal. This characteristically occurs when spindles from various animal cells are treated with concentrations of taxol greater than threshold values (Snyder and Mullins, 1993; Waters *et al.*, 1998), and we used it as a criterion when selecting cells for the laser microsurgical operations described below.

The effect of taxol on distribution of microtubules in the spindle was best resolved with polarized light (Figure 4, E–H). For the interpretation of images made with polarized light, white (maximal brightness) represents maximal retardance or birefringence; black represents no retardance or the absence of birefringence. Our images demonstrated that the taxol-induced broadening of the spindle poles correlated with greatly increased numbers and densities of microtubules that extended short distances (~2–3 μm) from the poles toward the equator. Microtubule densities in subpolar and equatorial domains after taxol treatment, however, did not appear to be different from those of controls. Spindle structure in those regions was especially important to this study. If taxol treatment had greatly altered the distribution of microtubules in those domains into which fragments were released after they had been severed from their chromosomes then any interpretation of fragment behavior would have to take those alterations into account. Because with the instrumentation we used the retardance magnitude within a given domain of the spindle is directly dependent on its microtubule number/density, we were able to quantify microtubules in those domains based on their retardance. We quantified retardance two ways: 1) within 0.55-μm^2 areas that were made within regions of interest (Figure 4, E and F), and 2) from line scans that were made along planes of interest (Figure 4, G and H). Taking those approaches, we found that retardance in central spindle domains (in the vicinities of chromosomes that could have

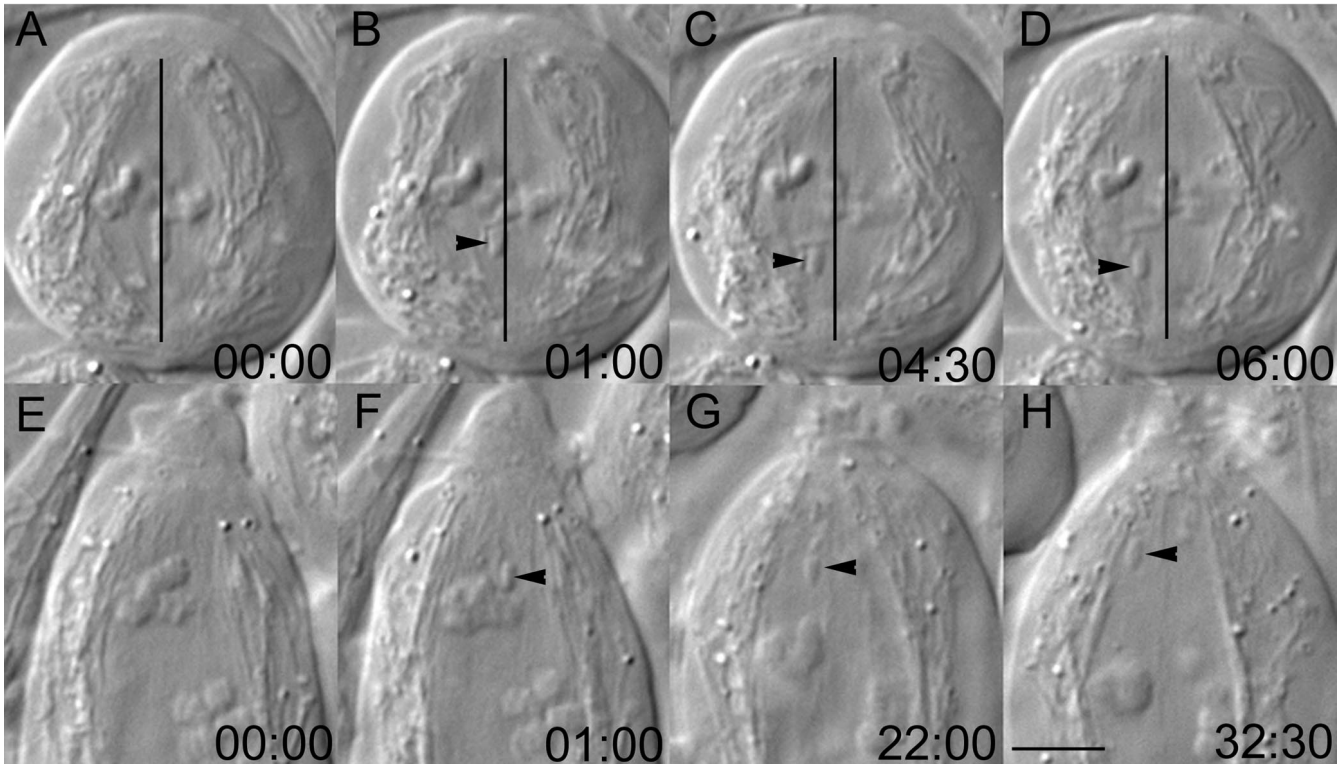

Figure 3. As the spindle forms during meiosis I and II, acentric fragments also experience a transverse force that eliminates them to the spindle periphery even as they are moving poleward. (A–D) Mid-prometaphase II cell in which a fragment, originally located near the spindle equator along the pole-to-pole axis (vertical line in B–D), moved laterally toward the spindle periphery as it migrated poleward. (E–H) Similar to A–D, except this fragment (F–H, arrow) was created near the spindle pole during prometaphase I. The fragment was slowly translated laterally toward the spindle periphery, which is outlined by a sheath of mitochondria. Bar (in H), 5 μm.

been cut had we been performing operations) in taxol-treated spindles was not significantly different (Student's *t* test, $p = 0.19$; differences were regarded significant at $p < .001$) from those in control spindles (Table 2). Our quantitative analysis revealed that retardance at spindle poles was clearly increased after taxol treatment, and a taxol effect also was manifested in reduced retardance of kinetochore fibers (Table 2). The latter suggests there are fewer microtubules per kinetochore in taxol, an effect also apparent from the data presented by Wilson and Forer (1997). The cause of this effect of taxol on kinetochore fibers is not known. One of the reviewers raised the possibility that the birefringence of kinetochore fibers in taxol is due to fewer than normal associated nonkinetochore microtubules in kinetochore fibers (Wise *et al.*, 1991). Data needed to confirm that, however, will require serial section electron microscopic analysis, such as that performed on untreated and cold-treated spermatocytes by Scarcello *et al.* (1986).

A final point regarding taxol effects on spermatocytes is that the doses of taxol that were effective in producing the taxol phenotype did not prevent entry into, or progression through, anaphase. For similar effects on spermatocytes from *Drosophila*, see Savoian *et al.* (2000). This was true for both meiosis I and II, but to obtain quantitative data on these points, analysis was restricted to spermatocytes in meiosis I. In the 83 untreated cells that we monitored, it took ~83 min on average to reach anaphase I onset after the breakdown of the nuclear envelope (NEB) at the end of diakinesis (Table 1). Spermatocytes from testes that had been incubated in 5 or 10 μM taxol for 15 min (see MATERIALS AND METHODS) progressed through meiosis in taxol, and the duration between NEB to anaphase I onset lasted somewhat longer, averaging 112 min over a range between 78 and 166 min (Table 1), yet in all 167 cells analyzed, the onset of anaphase was not prevented. In the time between NEB and anaphase, events usually seen in untreated cells, including congression of autosomes to the equator and metakinetic movements of sex univalents, were also observed in taxol-treated cells. We analyzed anaphase I in taxol-treated cells and found that segregating half-bivalents exhibited very slow (average velocity = 0.1 μm/min; range 0.1–0.3 μm/min; $n = 20$) poleward motion (Table 1). This was true in the cases of spindles that existed before taxol exposure and then shortened during exposure, as well as spindles that were assembled in taxol. Because this velocity was significantly less (Student's *t* test, $p < .0001$) than in untreated spermatocytes (0.5 μm/min; see above), anaphase A in taxol-shortened spindles lasted 30–40 min compared with 15 min in the longer spindles of controls (Figure 4, A–D).

The ultimate outcome of anaphase in the presence of taxol varied. In some cells chromosome poleward motion (anaphase A) was followed by elongation of the previously

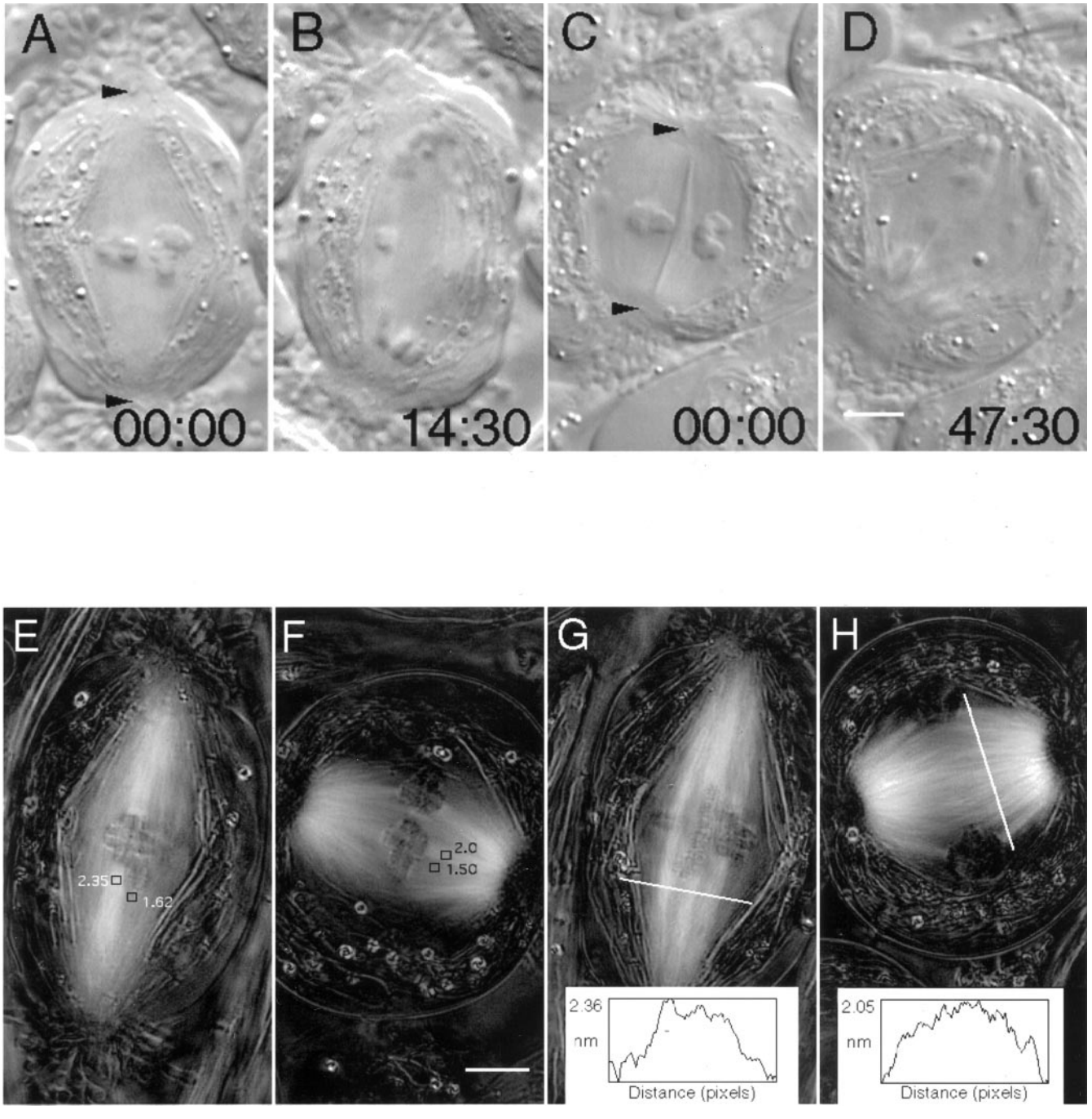

Figure 4. Taxol treatment induces the formation of short, broad spindles, but taxol does not inhibit anaphase onset or prevent the subsequent poleward motion of chromosomes. (A–D) Differential interference contrast micrographs of living DMSO (0.05%) control (A and B) and taxol (5 μM for 15 min)-treated (C and D) spermatocytes during meiosis I at metaphase (A and C) and near the completion of anaphase A (B and D). Positions of the basal bodies of the polar flagella are marked with arrowheads in A and C. Note that anaphase takes ~3 times longer in the shortened taxol spindle than in the DMSO control. Another noteworthy point, illustrated in C, is that mitochondria (normally restricted to the periphery of the spindle) often are found within the central domain of spindles formed in taxol. In this case, the mitochondrion appears as a highly refractile rod extending from pole to pole and between two bivalents. Time in minutes:seconds. Bar (in D), 5 μm. (E–H) Images generated with polarization microscopy depicting birefringence (bright contrast) due to spindle microtubules in untreated control (E and G) and taxol-treated (F and H) spermatocytes at metaphase. (E and F) Retardance magnitude was measured within areas 0.55 μm^2; kinetochore fiber retardance appears reduced after 5 μM taxol treatment (2.0 vs. 2.35 nm in the control; refer to Table 2 for summary), but nonkinetochore domains appear less affected by taxol (1.5 vs. 1.62 nm in the control). (G and H) Similar results were obtained from line scans made perpendicular to the spindle axis. The top of the line scan in H (10 μM taxol) is on the left of the plot. Bar (in F), 5 μm.

Table 2. Comparison of retardance magnitude in three spindle domains of control and taxol-treated spermatocytes

	Untreated control spermatocytes	0.1% DMSO control spermatocytes	Taxol-treated (5 and 10 μM, for 15 min) spermatocytes
Central spindle nonkinetochore microtubule domains[a]	1.8 nm (n = 13) (range: 1.2–2.4 nm)	1.9 nm (n = 9) (range: 1.6–2.4 nm)	1.6 nm (n = 17) (range: 1.1–2.5 nm)
Kinetochore fibers	2.2 nm (n = 4) (range: 1.9–2.4 nm)	1.9 nm (n = 2) (range: 1.7–2.2 nm)	1.5 nm (n = 6) (range: 1.2–2.1 nm)
Polar nonkinetochore microtubule domains	1.4 nm (n = 2) (range: 1.3–1.5 nm)	1.5 nm (n = 2) (range: 1.4–1.6 nm)	3.1 nm (n = 4)

[a] Retardance data were obtained from points within central spindle domains where arm-severing operations would have been performed with the laser microscope.

shortened spindle; those cells usually initiated, and sometimes completed, cytokinesis. In contrast, in other cells, the spindle poles moved progressively closer to one another during anaphase A, and this gradual collapse of the spindle inhibited the initiation of cytokinesis. It is noteworthy that neither congression nor anaphase was inhibited even when testes were incubated in 50 μM taxol for >30 min before spreading under oil.

Taxol Inhibits Poleward Transport of Acentric Chromosome Fragments during Metaphase

This part of our study was conducted only on meiosis I spermatocytes because, at the concentrations we used, taxol induced metaphase II half-spindles to become so short that meaningful studies were practically impossible. We found that the transport properties of meiosis I spindles were clearly and dramatically inhibited by taxol (Figure 5, C and D). Of the 24 acentric fragments generated in 24 prometaphase or metaphase I spermatocytes (Table 1), only two exhibited any pole-directed motion and the velocity of that motion (~0.1 μm/min) was greatly attenuated relative to controls. In those cells where the fragment exhibited no poleward motion, it was often slowly but progressively eliminated laterally toward the spindle periphery (Figure 5). In some cases the fragment was still contained within the spindle at anaphase onset and was observed to move poleward during anaphase within the interzone, usually trailing behind the segregating half-bivalents (Figure 5, E and G). When such poleward motion of fragments was observed during anaphase in taxol, their velocities, of course, were very slow (~0.1 μm/min).

DISCUSSION

The original goal of our study was to test the hypothesis that spindles in crane fly spermatocytes exert a pole-directed force on chromosomes independent of kinetochores. To do this we used laser microsurgery to sever the arms from metaphase chromosomes, between their kinetochore and telomere regions. We found that the resultant acentric fragments invariably moved poleward with a uniform velocity similar to that exhibited by kinetochores during anaphase. We also found that ribbons or sniglets of denatured material, generated anywhere within a half-spindle by laser irradiation, also moved poleward with the same kinetics. From these data we conclude that the production of kinetochore-independent, poleward forces is a general feature of crane fly spermatocyte half-spindles.

Poleward Transport of Acentric Fragments Is Mediated by Microtubule Flux

To uncover the mechanism underlying these forces, we treated spermatocytes with taxol before severing chromosome arms. In so doing, we have developed an indirect assay for microtubule flux. This approach should be useful on other cell types, for example, spermatocytes from other insect species or plant endosperm cells, which are not amenable to microinjection and therefore are precluded from direct analysis of flux by photoactivation of fluorescence (Mitchison, 1989) or fluorescent speckle microscopy (Waterman-Storer *et al.*, 1998).

Taxol rapidly inhibits microtubule flux within spindles. It does not affect the activity of microtubule-based motors (Vale *et al.*, 1985), and thus it provided the means for distinguishing between possible flux-based and motor-based mechanisms of arm fragment transport. At low concentrations taxol preferentially inhibits microtubule plus end dynamics in vitro and in vivo, whereas at higher concentrations both plus and minus ends are affected (Jordan *et al.*, 1993; Derry *et al.*, 1995). When vertebrate somatic cells are treated with 10 μM taxol during metaphase, microtubule subunit incorporation at the kinetochores is inhibited well before removal at the poles (Waters *et al.* 1996). Because of this differential inhibition, the kinetochore microtubules shorten as subunits are lost at the poles, and the spindle shortens as the poles hold on to shortening microtubules attached to the chromosomes (Waters *et al.*, 1996; Derry *et al.*, 1998).

We found that the spermatocytes obtained from testes treated with 5 or 10 μM taxol for 15 min contained significantly shortened spindles characteristic of the taxol phenotype (Table 2; Wilson and Forer, 1997). When we generated acentric chromosome fragments near the spindle equator in these cells, they failed to move poleward, or they displayed significantly attenuated poleward motion (~0.1 μm/min vs. ~0.5 μm/min in controls). The two fragments that exhibited this motion were likely generated in spindles in which the effects of taxol had not yet been fully reached.

Taxol promotes microtubule assembly (Schiff *et al.*, 1979), and it was possible that an increase in microtubule density within each half-spindle impeded the poleward motion of

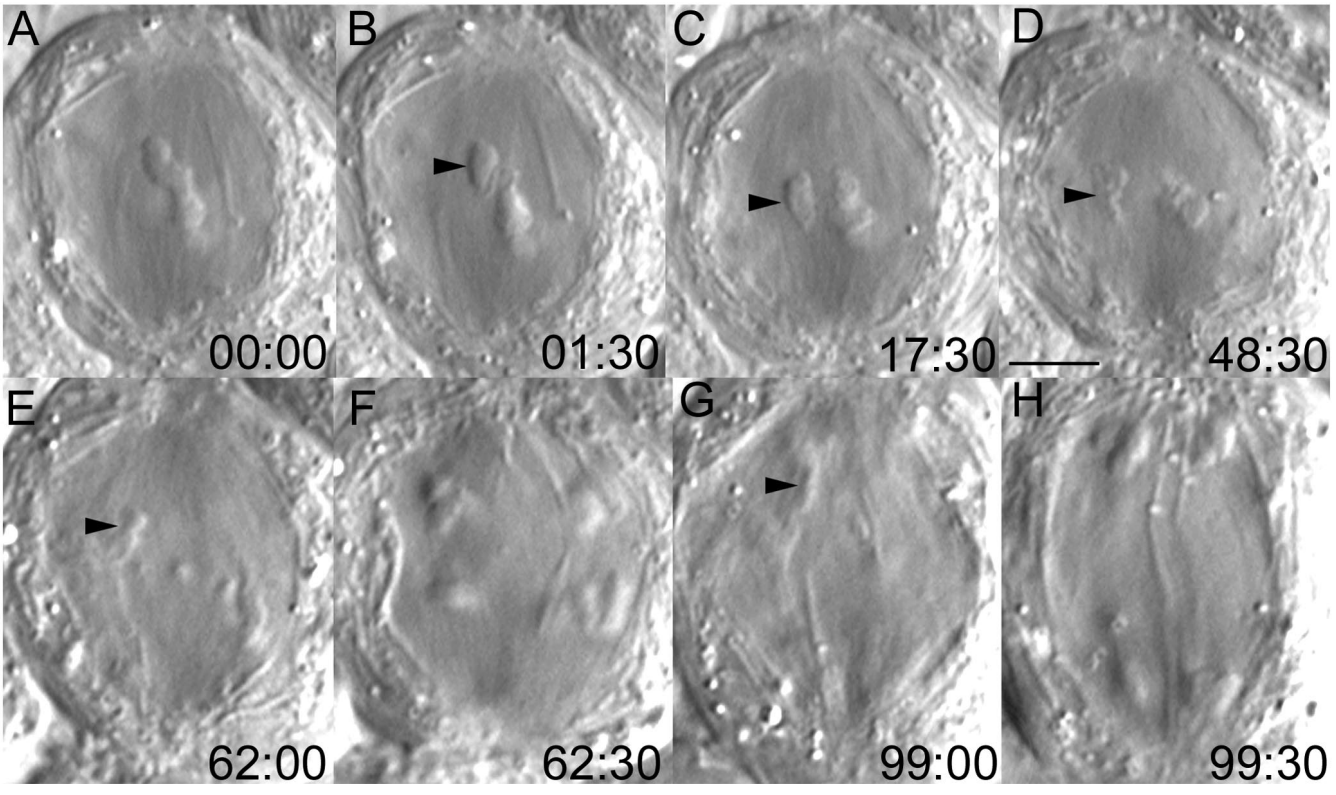

Figure 5. Acentric fragments, generated near the spindle equator in taxol-treated spermatocytes, are not transported poleward as they are in control spermatocytes. (A–H) Selected frames from a time-lapse sequence of a taxol-treated primary spermatocyte that contained a pole-directed achiasmic arm (A–D, arrowhead). After it was severed with the laser (B), this arm remained relatively motionless over the next 47 min until it began to disintegrate before anaphase onset. (E–H) During anaphase, the fragment disintegrated further as it moved poleward (E and G), trailing behind the segregating half-bivalents (F and H), which moved poleward with a velocity of ~ 0.1 μm/min. Time in minutes:seconds. Bar (in D), 5 μm.

acentric fragments. To evaluate this, we used quantitative polarization microscopy to determine the density of microtubules within those areas of taxol-treated spindles where fragments were released by our cutting operations. We found that taxol treatment did not significantly increase the density of microtubules in those regions, although it did enhance microtubule density near the spindle poles.

From these results, we conclude that the force for transporting acentric chromosome fragments and the other material poleward in crane fly spermatocytes is produced by microtubule flux. Chromosome arms must simply become trapped by the dense arrays of microtubules in the half-spindle (LaFountain 1974, 1976; Scarcello *et al*., 1986) and then are directed poleward as their surfaces interact with fluxing microtubules. This conclusion provides a ready explanation for why areas of reduced birefringence, created on crane fly spermatocyte kinetochore fibers by UV irradiation, move poleward (Forer, 1966). It also reveals that the transport properties of crane fly spermtocyte spindles are similar to metaphase spindles in plant endosperm (Khodjakov *et al*., 1996) but differ from those of animal somatic cells in which a polar wind is generated by microtubule plus end-directed motors associated with chromosome arms (Rieder and Salmon, 1994).

During Anaphase, Kinetochore Microtubules Depolymerize at Their Minus Ends

Our assay reveals that acentric chromosome fragments also moved poleward during anaphase with the same velocities exhibited by chromosomes (~0.5 μm/min). Because the rate of flux during metaphase is similar to the rate of chromosomes during anaphase, a flux-based mechanism, involving shortening of kinetochore microtubules at their minus ends, is implicated for anaphase. Thus, our data independently confirm the conclusion of Wilson *et al.* (1994). By taking advantage of the fact that kinetochore microtubules in crane fly spermatocytes are acetylated, except for an unacetylated "gap" near kinetochores (Wilson and Forer, 1989), they were able to show that at least 80% of the shortening of kinetochore fibers during anaphase is due to subunit removal at the pole.

Although the rate at which kinetochores move poleward during anaphase in taxol-treated spermatocytes is reduced by 80% (from 0.5 μm/min to only ~0.1 μm/min), the chromosomes invariably completed this migration. Why and how this occurs is unclear. It is possible that our taxol treatment did not eliminate flux. That is, it did not completely inhibit the incorporation of microtubule subunits at

kinetochores and their removal at the poles. However, our observation that the majority of acentric fragments generated in metaphase cells failed to exhibit poleward motion suggests that in most cases flux is shut down completely by the time of anaphase onset. The idea that subunit incorporation into kinetochore microtubules is inhibited, but that some residual removal at the pole continues, is not consistent with our finding that taxol-treated spindles reached an equilibrium length after which they no longer shortened. In their study on the sites of microtubule disassembly during anaphase in crane fly spermatocytes, Wilson *et al.* (1994) concluded that although 80% of kinetochore fiber shortening occurs by subunit removal at the pole, 20% can be attributed to subunit removal at the kinetochore. Thus, it is possible that the stability of kinetochore microtubule plus ends is suddenly modified at anaphase onset in taxol-treated cells by, for example, the rapid inactivation of the CDK1 kinase, which then allows them to shorten by subunit removal at the kinetochore.

Our conclusion that anaphase chromosome motion in crane fly spermatocytes is driven primarily by flux differs from Nicklas' (1989) finding that in grasshopper spermatocytes the force for poleward chromosome motion during anaphase is generated at or near the kinetochores and that during this motion microtubules shorten primarily by subunit removal at kinetochores. Recent work on *zw10* and *rod* mutants also suggests that the force for anaphase motion in *Drosophila* spermatocytes is generated primarily at the kinetochore (Savoian *et al.*, 2000; Sharp *et al.*, 2000). Together, these studies imply that the relative contribution that each (redundant) force-producing mechanism contributes to moving chromosomes poleward during meiosis in insect spermatocytes varies between organisms.

CONCLUSION

Our findings add to the growing body of evidence in support of the conclusion that both kinetochore-based and flux-based mechanisms exist and that the mechanism that is emphasized depends on the particular system. Although flux is a contributor in animal somatic cells, forces produced by kinetochore-associated motors, or disassembling microtubule plus ends, appear to dominate (Mitchison and Salmon, 1992; Zhai *et al.*, 1995). Here we show that each of the two opposing half-spindles in crane fly spermatocytes are "flux machines" that transport kinetochores, acentric chromosome fragments, and other inclusions poleward as they adhere to the surfaces or plus ends of microtubules. These spindles are therefore similar to those formed in *Xenopus* oocyte extracts (Murray *et al.*, 1996; Desai *et al.*, 1998) in that the force for poleward chromosome motion is also produced by microtubule flux as kinetochore microtubules shorten by subunit removal at the pole.

In such flux machines, "slippage" must occur between the plus ends of kinetochore microtubules and the kinetochores during metaphase, when poleward motion is prevented by the cohesion of homologs (or sister chromatids). As the machine continues to flux, this slippage, which in vertebrate somatic cells produces a "neutral" kinetochore state (Khodjakov and Rieder, 1996), could still maintain the tension on the kinetochores needed to stabilize attachment to the spindle (Nicklas, 1997). Then, when the chromosomes disjoin at anaphase onset, the sudden decrease in tension could release the clutch on the opposing kinetochores, engage the gears (i.e., stop slippage), and allow the force produced by flux to move the chromosome poleward.

Although the molecular basis for flux is unknown, it has been proposed that microtubule plus end-directed motors, anchored within the spindle matrix, could push the microtubule lattice toward the spindle pole (Sawin and Mitchison, 1991). An actin/myosin system located within the kinetochore fiber and spindle matrix could act in a similar manner (Waterman-Storer and Salmon, 1997; Silverman-Gavrila and Forer, 2000). Regardless of the mechanism, the flux-mediated production of forces for kinetochore poleward motion is compatible with traction fiber models (reviewed by Hays and Salmon, 1990) for chromosome positioning. In this view chromosomes become aligned on the spindle equator because the opposing poleward "pulling" forces, acting on sister kinetochores, are proportional to the length of the kinetochore fibers. Challenges for the future will be to determine whether chromosome congression in flux machines is indeed mediated by traction fibers and how poleward forces that act on the chromosome arm influence this process.

ACKNOWLEDGMENTS

We gratefully acknowledge the contributions made to this study by A. Khodjakov, G. Rickards, S. Inoué, K. LaFountain, D. LaFountain, and A. Siegel. We also thank the reviewers who recommended revisions that improved the final version of this report. This research was supported by grants from the National Science Foundation (MCB-9808290 to J.L.) and National Institutes of Health (GM-40198 to C.R. and GM-49210 to R.O). Much of the work was completed in the Video LM Core Facility of the Wadsworth Center.

REFERENCES

Adames, K.A., and Forer, A. (1996). Evidence for poleward forces on chromosome arms during anaphase. Cell Motil. Cytoskeleton *34*, 13–25.

Antonio, C., Ferby, I., Wilhelm, H., Jones, M., Karsenti, E., Nebreda, A.R., and Vernos, I. (2000). Xkid, a chromokinesin required for chromosome alignment on the metaphase plate. Cell *102*, 425–435.

Begg, D.A., and Ellis, G.W. (l979). Micromanipulation studies of chromosome movement. II. Birefringent chromosomal fibers and the mechanical attachment of chromosomes to the spindle. J. Cell Biol. *82*, 542–554.

Cole, R.W., Khodjakov, A., Wright, W.H., and Rieder, C.L. (1995). A differential Interference contrast-based light microscopic system for laser microsurgery and optical trapping of selected chromosomes during mitosis *in vivo*. J. Microsc. Soc. Am. *1*, 203–215.

Derry, W.B., Wilson, L., and Jordan, M.A. (1995). Substoichiometric binding of taxol suppresses microtubule dynamics. Biochemistry *34*, 2203–2211.

Derry, W.B., Wilson, L., and Jordan, M.A. (1998). Low potency of taxol at microtubule minus ends: implications for its antimitotic and therapeutic mechanism. Cancer Res. *58*, 1177–1184.

Desai, A., Maddox, P.S., Mitchison, T.J., and Salmon, E.D. (1998). Anaphase A chromosome movement and poleward spindle microtubule flux occur at similar rates in *Xenopus* extract spindles. J. Cell Biol. *141*, 703–713.

Forer, A. (1966). Characterization of the mitotic traction system and evidence that birefringent spindle fibers neither produce not transmit force for chromosome movement. Chromosoma *19*, 44–98.

Funabiki, H., and Murray, A.W. (2000). The *Xenopus* chromokinesin Xkid is essential for metaphase chromosome alignment and must be degraded to allow anaphase chromosome movement. Cell *102*, 411–424.

Hays, T.S., and Salmon, E.D. (1990). Poleward force at the kinetochore in metaphase depends on the number of kinetochore microtubules. J. Cell Biol. *110*, 391–404.

Hoffman, D.B., Pearason, C.G., Yen, T.J., Howell, B.J., and Salmon, E.D. (2001). Microtubule-dependent changes in assembly of microtubule motor proteins and mitotic spindle checkpoint proteins at PtK_1 kinetochores. Mol. Biol. Cell *12*, 1995–2009.

Inoué, S., and Salmon, E.D. (1995). Force generation by microtubule assembly/disassembly in mitosis and related movements. Mol. Biol. Cell *6*, 1619–1640.

Janicke, M.A., and LaFountain, J.R., Jr. (l986) Bivalent orientation, and behavior in crane-fly spermatocytes recovering from cold exposure. Cell Motil. Cytoskeleton *6*, 492–501.

Jordan, M.A., Toso, R.J., Thrower, D., and Wilson, L. (1993). Mechanism of mitotic block and inhibition of cell proliferation by taxol at low concentrations. Proc. Natl. Acad. Sci. USA *90*, 9552–9556.

Khodjakov, A., Cole, R.W., Bajer, A.S., and Rieder, C.L. (1996). The force for poleward chromosome motion in *Hemanthus* cells acts along the length of the chromosome during metaphase but only at the kinetochore during anaphase. J. Cell Biol. *132*,1093–1104.

Khodjakov, A., and Rieder, C.L. (1996). Kinetochores moving away from their associated pole do not exert a significant pushing force on the chromosome. J. Cell Biol. *135*, 315–327.

LaFountain, J.R. (1972). An association between microtubules and aligned mitochondria in *Nephrotoma* spermatocytes. Exp. Cell Res. *71*, 325–328.

LaFountain, J.R. (1974). Birefringence and fine structure of spindles in spermatocytes of *Nephrotoma suturalis* at metaphase of the first meiotic division. J. Ultrastruct. Res. *46*, 268–278.

LaFountain, J.R. (1976). Analysis of birefringence and ultrastructure of spindles in primary spermatocytes of *Nephrotoma suturalis* during anaphase. J. Ultrastruct. Res. *54*, 333–346.

LaFountain, J.R., Jr., Siegel, A.J., and Rickards, G.K. (1999). Chromosome movement during meiotic prophase in crane-fly spermatocytes. IV. Actin and the effects of cytochalasin D. Cell Motil. Cytoskeleton *43*, 199–212.

Mitchison, T.J. (1989). Polewards flux in the mitotic spindle: evidence from photoactivation of fluorescence. J. Cell Biol. *109*, 637–652.

Mitchison, T., Evans, L., Schulze, E., and Kirschner, M. (1986). Sites of microtubule assembly and disassembly in the mitotic spindle. Cell *45*, 515–527.

Mitchison, T.J., and Salmon, E.D. (1992). Poleward kinetochore fiber movement occurs during both metaphase and anaphase A in newt lung cell mitosis. J. Cell Biol. *119*, 569–582.

Mitchison, T.J., and Sawin, K.E. (1990). Tubulin flux in the mitotic spindle: where does it come from, where is it going? Cell Motil. Cytoskeleton *16*, 93–98.

Murray, A.W., Desai, A.B., and Salmon, E.D. (1996). Real time observation of anaphase *in vitro*. Proc. Natl. Acad. Sci. USA *93*, 12327–12332.

Nicklas, R.B. (1989). The motor for poleward movement in anaphase is in or near the kinetochore. J. Cell Biol. *109*, 2245–2255.

Nicklas, R.B. (1997). How cells get the right chromosomes. Science *275*, 632–637.

Oldenbourg, R., and Mei, G. (1995). New polarized light microscope with precision universal compensator. J. Microsc. *180*, 140–147.

Östergren, G. (1945). Transverse equilibria on the spindle. Botaniska Notisek *4*, 467–468.

Pfarr, C.M., Coue, M., Grisson, M., Hays, T.S., Porter, M.E., and McIntosh, J.R. (1990). Cytoplasmic dynein is localized to kinetochores during mitosis. Nature *345*, 263–265.

Pickett-Heaps, J.D., Forer, A., and Spurck, T. (1996). Rethinking anaphase: where "Pac-man" fails and why a role for the spindle matrix is likely. Protoplasma *192*, 1–10.

Rieder, C.L., and Salmon, E.D. (1994). Motile kinetochores and polar ejection forces dictate chromosome position on the vertebrate mitotic spindle. J. Cell Biol. *124*, 223–233.

Savoian, M.S., Goldberg, M.L., and Rieder, C.L. (2000). The rate of poleward chromosome motion is attenuated in *Drosophila zw10* and *rod* mutants. Nat. Cell Biol. *2*, 948–952.

Sawin, K.E., and Mitchison, T.J. (1991). Poleward microtubule flux in mitotic spindles assembled *in vitro*. J. Cell Biol. *112*, 941–954.

Scarcello, L.A., Janicke, M.A., and LaFountain, J.R. (1986). Kinetochore microtubules in crane-fly spermatocytes: untreated, 2°C treated, and 6°C grown spindles. Cell Motil. Cytoskeleton *6*, 428–438.

Schiff, P.B., Fant, J., and Horwitz, S.B. (1979). Promotion of microtubule assembly *in vitro* by taxol. Nature *277*, 665–667.

Sharp, D.J., Rogers, G.C., and Scholey, J.M. (2000). Cytoplasmic dynein is required for poleward chromosome movement in *Drosophila* embryos. Nat. Cell Biol. *2*, 922–930.

Silverman-Gavrila, R.V., and Forer, A. (2000). Evidence that actin and myosin are involved in the poleward flux of tubulin in metaphase kinetochore microtubules of crane-fly spermatocytes. J. Cell Sci. *113*, 597–609.

Snyder, J.A., and Mullins, J.M. (1993). Analysis of spindle microtubule organization in untreated and taxol-treated PtK1 cells. Cell Biol. Int. *17*, 1075–1084.

Steurer, E.R., Wordeman, L., Schroer, T.A., and Sheetz, M.P. (1990). Localization of cytoplasmic dynein to mitotic spindles and kinetochores. Nature *345*, 266–268.

Tucker, J.B. (1977). Shape and pattern specification during microtubule bundle assembly. Nature *266*, 22–26.

Vale, R.D., Schnapp, B.J., Mitchison, T., Steuer, E., Reese, T.S., and Sheetz, M.P. (1985). Different axoplasmic proteins generate movement in opposite directions along microtubules *in vitro*. Cell *43*, 623–632.

Waterman-Storer, C.M., Desai, A., Chloe Bulinski, J., and Salmon, E.D. (1998). Fluorescent speckle microscopy, a method to visualize the dynamics of protein assemblies in living cells. Curr. Biol. *8*, 1227–1230.

Waterman-Storer, C.M., and Salmon, E.D. (1997). Actomyosin-based retrograde flow of microtubules in the lamella of migrating epithelial cells influences microtubule dynamic instability and turnover and is associated with microtubule-breakage and treadmilling. J. Cell Biol. *139*, 417–434.

Waters, J.C., Chen, R.-H., Murray, A.W., and Salmon, E.D. (1998). Localization of Mad2 to kinetochores depends on microtubule attachment, not tension. J. Cell Biol. *141*, 1181–1191.

Waters, J.C., Mitchison, T.J., Rieder, C.L., and Salmon, E.D. (1996). The kinetochore microtubule minus-end disassembly associated with poleward flux produces a force that can do work. Mol. Biol. Cell *7*, 1547–1558.

Wilson, P.J., and Forer, A. (1989). Acetylated α-tubulin in spermatogenic cells of the crane fly *Nephrotoma suturalis*: kinetochore microtubules are selectively acetylated. Cell Motil. Cytoskeleton *14*, 237–250.

Wilson, P.J., and Forer, A. (1997). Effects of nanomolar taxol on crane-fly spermatocyte spindles indicate that acetylation of kinetochore microtubules can be used as a marker of poleward tubulin flux. Cell Motil. Cytoskeleton *37*, 20–32.

Wilson, P.J., Forer, A., and Leggiadro, C. (1994). Evidence that kinetochore microtubules in crane-fly spermatocytes disassemble during anaphase primarily at the poleward end. J. Cell Sci. *107*, 3015–3027.

Wise, D., Cassimeris, L., Rieder, C.L., Wadsworth, P., and Salmon, E.D. (1991). Chromosome fiber dynamics and congression oscillations in metaphase PtK_2 cells at 23°C. Cell Motil. Cytoskeleton *18*, 131–142.

Zhai, Y., Kronebusch, P.J., and Borisy, G.G. (1995). Kinetochore microtubule dynamics and the metaphase-anaphase transition. J. Cell Biol. *131*, 721–734.